

Detection Limits of Optical Gas Imaging for Natural Gas Leak
Detection in Realistic Controlled Conditions
Supplementary Information

Daniel Zimmerle¹, Timothy Vaughn¹, Clay Bell¹, Kristine Bennett¹, Parik Deshmukh², and Eben Thoma³

¹Energy Institute, Colorado State University, Fort Collins, CO, USA

²Jacobs Technology, Durham, North Carolina

³EPA Office of Research and Development, Durham North Carolina

July 3, 2020

Contents

| | | |
|------------|---|------------|
| S-1 | Facility | S3 |
| S-2 | Methods | S4 |
| S-2.1 | Metering and Calibration | S4 |
| S-2.2 | Self-Reported Operator Data | S5 |
| S-2.3 | Testing Process | S5 |
| S-2.4 | Data Added Post-Testing | S6 |
| S-2.5 | Statistical Methods | S9 |
| S-3 | Test Conditions | S10 |
| S-4 | Detection Curves and Comparison to Ravikumar et al. | S17 |
| S-5 | Experience Analysis | S17 |
| S-6 | Affiliation Analysis | S23 |
| S-7 | Other Variables | S26 |
| S-8 | Videos | S29 |
| S-8.1 | SI Video 1: Varying Conditions, Auto and HSM Modes | S29 |
| S-8.2 | SI Video 2: Varying Conditions in HSM Mode | S29 |
| S-8.3 | SI Video 3: Variation in Background | S30 |
| S-8.4 | SI Video 4: Same Leak, Three Observation Directions | S30 |
| S-8.5 | SI Video 5: Method Interference in HSM Mode | S30 |
| S-9 | Data Dictionary | S31 |

List of Figures

| | | |
|------|---|-----|
| S-1 | Aerial view of the test site. | S3 |
| S-2 | the Methane Emissions Technology Evaluation Center (METEC) gas release system schematic | S5 |
| S-3 | Calendar distribution of test days | S10 |
| S-4 | Weather conditions during testing | S11 |
| S-5 | Daily variation in wind speeds | S12 |
| S-6 | Emission rate distribution. | S13 |
| S-7 | Emission rates by equipment type | S13 |
| S-8 | Detection rate by emission point ID | S14 |
| S-9 | Detection rate for each emission point | S14 |
| S-10 | Survey time by pad | S15 |
| S-11 | Surveyor experience | S18 |
| S-12 | Detection rate for individual surveyors | S19 |
| S-13 | Detection rate histograms for experience groupings | S20 |
| S-14 | Detection rate by experience and wind speed | S21 |
| S-15 | Detection rate by hour of day | S21 |
| S-16 | Detection rate by equipment type | S22 |
| S-17 | Detection distance for compliance and LDAR surveyors | S23 |
| S-18 | Detection rate by hour of day by affiliation | S24 |
| S-19 | Detection rate by equipment type by affiliation | S25 |
| S-20 | Impact of wind speed and emission rate on detection | S26 |
| S-21 | Time spent by experience level | S27 |
| S-22 | Summary of detected emissions | S28 |
| S-23 | Labeled view of a separator enclosure | S31 |

List of Tables

| | | |
|-----|--|-----|
| S-1 | Well Pad Summary | S3 |
| S-2 | Emission Point Primary and Secondary Backgrounds | S8 |
| S-3 | Emission Point Primary Background | S9 |
| S-4 | Emission Point Characteristics | S16 |
| S-5 | 90% Probability-of-Detection Rates | S17 |
| S-6 | Fraction of Reports by Affiliation and Experience | S18 |
| S-7 | Groupings for Experience Cutoff Sensitivity Analysis | S20 |

S-1 Facility

The METEC facility was constructed under award from the Advanced Research Project Agency – Energy (ARPA-E) Methane Observation Networks with Innovative Technology to Obtain Reductions (MONITOR) program. METEC includes five mock well pads on a dedicated eight-acre site. These five pads were configured into three testing pads for the purposes of this study, as shown in Figure S-1.

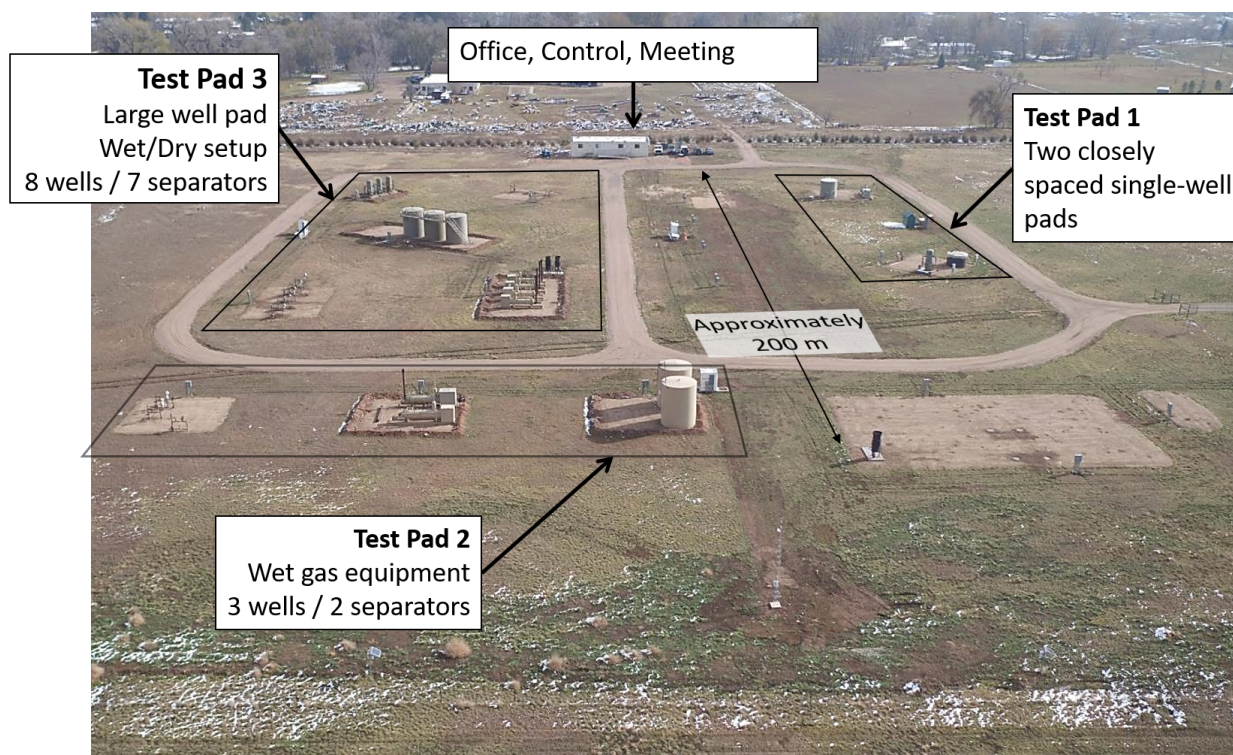


Figure S-1: Aerial view of the METEC at Colorado State University (CSU), as it was configured for the testing. Equipment was divided into three “well pads”, as indicated, each including wellheads, separators (equipment that separates liquids from gases during production), and tanks for storing liquids. The entire facility covers approximately 8 acres (3.2 ha), and the loop road encloses an area approximately 130 x 130 meters.

Table S-1 provides an overview of the equipment on each pad.

Table S-1: Well Pad Summary

| Pad ID | Well Head Count | Separator Count | Tank Count | Notes |
|--------|-----------------|-----------------|------------|--|
| 1 | 2 | 2 | 2 | Two simple well pads, spread some distance apart |
| 2 | 3 | 2 | 2 | Cluster of three well heads, 2 wet gas separators, 2 tanks |
| 3 | 8 | 7 | 3 | Large pad with 8 well heads in two groups |

The natural gas production equipment was donated to CSU by member companies in the

METEC Industry Advisory Board (IAB) during the facility's construction. No liquids were kept in the tanks or separators and none of the production piping was pressurized. Natural gas for emission locations was routed to release points using small diameter rigid or flexible tubing. Where possible tubing was hidden within the equipment, or utilized existing small diameter tubing to route gas to emission points.

Equipment (wellheads, separators, and liquid storage tanks) were arranged to represent well pads with the spacing and orientation of equipment taken from operational well pads that had been visited by CSU personnel at some point during the the previous three years. METEC implements a total of over 200 above-ground controlled release locations – not all of which were on the equipment used for this study – and could simulate steady-state and intermittent emissions similar to routine venting (e.g. pneumatic actuators) and fugitive leaks (e.g. flanges, fittings, and valves). While most release locations were above ground, one underground location near the wells on a well pad was also included in the study.

Weather conditions were recorded using a 6-meter, stationary, weather station at the west end of the facility, near Pad 3. Gas composition was measured using an on-site gas chromatograph.

S-2 Methods

All testing was completed under U.S. Environmental Protection Agency (EPA) Quality Assurance Program Plan: OGI Performance Studies, QAPP-2J17-013.0, Revision 0, December 4, 2017, EPA QA Track number G-AEMD-0031350. Key appendices are attached as supplementary material and referenced in this document.

S-2.1 Metering and Calibration

Emission sources were controlled and metered using the METEC gas release system, shown in Figure S-2. Gas was provided at a regulated pressure from a gas cylinder (1). The gas flow was divided and each primary branch was metered using an OMEGA FMA-17xx series thermal mass flow meter (2). Each primary branch was further divided into secondary branches where pressure regulators allowed the pressure of each secondary line to be independently controlled (3). Each secondary line provided gas at a regulated pressure to an orifice-based flow controller (4). Flow controllers adjusted emission rates by opening valves in-line with different orifice sizes. Emission points connected to the controller outlets are individually controlled by the system (5).

When multiple emission sources were controlled downstream of a single flow meter, a pretest calibration procedure was used to determine the flow rate of each individual emission source. During this procedure, each emission source was operated and metered individually. This metered emission rate was then assigned to the emission point during the test.

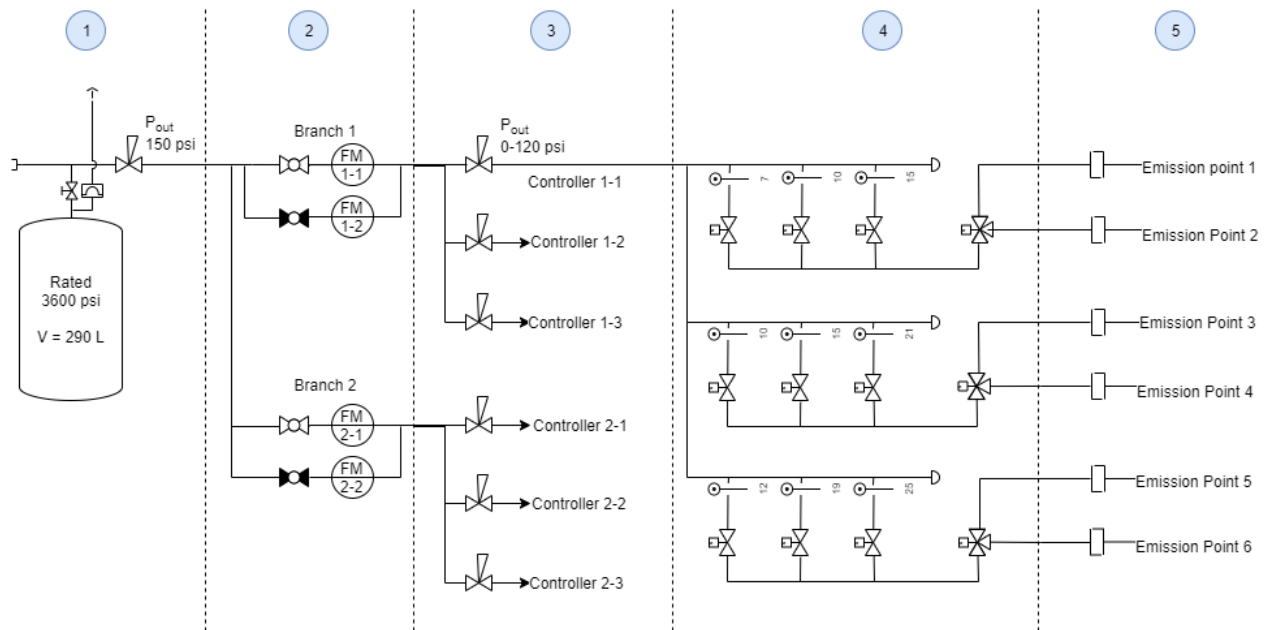


Figure S-2: METEC gas release system schematic. See text for description of the operation.

S-2.2 Self-Reported Operator Data

Camera operators who participated in the study each completed a questionnaire describing their experience level and specifics about the camera used during testing. The questionnaire is included as supplementary information in the file *QAPP Appendix C & D.pdf*. It included data on the approximate number of facilities the operator had performed OGI surveys on, the number of OGI surveys the surveyor had performed, and the training or certification the operator had received.

S-2.3 Testing Process

Testing was completed in “rounds” where each round consisted of a single test configuration, including all three pads. In the data tables, a test configuration can be identified by its *TestID*, a ‘round’ can be identified by the tuple consisting of the *TestID* and the date on which the test was conducted. Typically multiple surveyors, potentially accompanied by assistants to record observations, participated in each round. To anonymize participants, each organization that sent surveyors was assigned a random two-letter code (e.g. *PY*), and each surveyor from that organization was assigned a number (e.g. *PY1*).

Each round was performed according to the following procedure:

- All surveyors started inside the METEC office and completed the *OGI Information Survey Form* in *QAPP Appendix C & D.pdf*. Data from these forms is included in *OGIDataTables.xlsx* in sheet *D1 SurveyorData*.
- METEC staff configured the facility for the upcoming test based upon pre-determined plans:

- Pressure setpoints were set at the release controller for each test pad.
 - Any manual valves were adjusted for the desired test configuration following METEC internal piping diagrams
 - METEC staff ran the pretest calibration procedure to meter all emission sources individually.
 - The test configuration was switched into operating mode for surveys
- Surveyors surveyed each pad in an assigned order:
 - Surveyors started on their assigned pad, surveyed all components on that pad, and then moved to the next pad, in assigned order.
 - Surveyors recorded each emission source they found on a detection log. A blank example is provided in the supplementary information in file *QAPP Appendix C & D.pdf*.
 - Surveyors were instructed to not observe other surveyors, and to not enter pads where another surveyor was active, with the exception that Pad 3 was divided into two sections (east and west of the tank battery), and surveyors were allowed to be in each section simultaneously.
 - In a minority of surveys, a surveyor interrupted the survey before completing all pads (e.g. for lunch), and then completed the survey later. Similarly, in a few instances, a surveyor skipped part of one pad – most often because another surveyor was on the pad – and then returned to the pad later to complete the survey. In either of these cases, the duration of the survey was adjusted to omit the time away from the pad.
 - Operators returned to the METEC control center and submitted their test log to METEC staff.
 - At the request of the surveyors, when all surveyors had completed their survey, METEC staff provided the surveyors with feedback on the number of emission points on the site, but did not tell surveyors the location of the emissions (to protect confidentiality for subsequent surveyors). As a result, surveyors received some minimal feedback on their detection rate during the day, but *not* during any one test configuration.
 - After testing was complete, METEC staff entered detection data from the paper detection logs and scanned the logs for later reference. Detection data, included data added post-testing, is included in *OGIDataTables.xlsx* in sheet *D3 Data*.

Most analyses presented here and in the main paper defined a test as the combination of one test configuration, on one pad, screened by one surveyor, on one day. Individual tests can be identified in the data files by the *ConfigID* field, which is a concatenation of operator ID (*OpID*), test ID (*TestID*), pad ID (*PadID*), and a number indicating day of the year (e.g. *PY1-T1-P3-29*).

S-2.4 Data Added Post-Testing

Following testing, additional data was added to each emission point used in the test, including the angle of view, background, etc. – see Section S-3 for definitions. These data are included in the data file, *OGIDataTables.xlsx*, as sheet *D2 LeakPointData*.

Every row in the data file is a *test* – i.e. a single opportunity for a surveyor to find a non-zero emission or to identify a non-emitting well pad as having no emissions. Fields in the data file may be utilized to subset and count tests and compute detection rates. However, special care is required to define the role of false positives when calculating detection or error rates. We do this by defining two forms of testing:

First, there are *defined* tests where the surveyor screened a well pad with no emissions, and may either have indicated no emissions (a true negative) or may have indicated incorrectly that there were emissions (a false positive). We treat these cases as a single *defined* test case: the surveyor is presented with a set of equipment with no emissions, and may report one or more leaks. *Any* leak report is considered *one* false positive and represents one defined test case. If the surveyor found identified multiple emission points, these are noted as multiple locations in the `LocationDescription` field.

Second, there is a set of tests – both defined and undefined – where a surveyor screened a well pad with one or more emission points, and may have correctly identified some (true positives), missed some (false negatives), and/or identified emission locations where no emissions occurred (false positives). When there are non-zero emissions on the pad, false positives are uncontrolled results – the surveyor could find any number of extra (or mis-located) emission points, and each represents a detection error relative to the challenge presented to the surveyor – i.e. find the actual leaks. In this case, the number of *defined* tests is the number of emission points, not including false positives, and the number of total test results includes all results, including the false positives. Therefore, the number of “tests” in the file exceeds the number of “defined tests” used for the study.

There are many more tests (415) in the second form of testing - finding non-zero leaks – than in the first – detecting a non-leaking well pad (73 tests).

The logic to extract subsets from the data set is defined below, in the form `V:=equation`, where `V` is a subset of all tests, and `equation` is the required statement to identify each row (test) as being part of that subset of tests. The equations reference column headers in the data file.

- `NoLeak:=NoLeakTest=='Yes'` – A test where there were no emissions released on a pad. Tests in this category can be true negatives (TN) and false positives (FP).
- `LeakTest:=NoLeakTest=='No'` – A test where there were emissions to be detected *somewhere* on the well pad where the test was performed. Tests in this category can be true positives (TP), false negatives (FN), or false positives (FP).
- `ZeroTest:=NoLeak` – All *defined* tests where a surveyor tried to detect emissions on a well pad with no emission points, which is the same as `NoLeak`. These are null emission test cases and results are either true negatives (TN) or false positives (FP). The “zero confirmation rate” is a pad-level metric on how frequently surveyors properly indicate a non-emitting pad was non-emitting:

$$R_z = \frac{\text{count}(TN)}{\text{count}(ZeroTest)} \quad (1)$$

- `NonZeroTest:=LeakTest and Detected != 'FP'` – All *defined* tests where surveyors tried to detect at least one non-zero emission on one well pad. These include `LeakTest` tests minus

false positives occurring on pads where there were other emissions. This group represents true detection opportunities and results are either true positives (TP) or false negatives (FN). Detection rate is

$$R_d = \frac{\text{count}(TP)}{\text{count}(NonZeroTest)} \quad (2)$$

- **DefinedTest:=ZeroTest or NonZeroTest** – All defined tests of any type. Every row in the data set is a **DefinedTest** minus false positives found on a well pad where there were other emission points; the false positives are undefined extra detections on pads with other emitters. The total positive performance of any set of surveyors is the total successful outcomes, divided by the total number of defined tests:

$$R_t = \frac{\text{count}(TP) + \text{count}(TN)}{\text{count}(NonZeroTest) + \text{count}(ZeroTest)} \quad (3)$$

This metric is infrequently used because the number of **ZeroTests** is much smaller than the number of **NonZeroTests**, and therefore $R_t \approx R_d$.

The background normally seen when screening a leak was determined by viewing the leak from a normal standing position and noting the background behind the leak. The surveyor for this classification was ≈ 6 feet tall and used an OpGal™EyeCGas® camera. The surveyor was familiar with the facility and approached the leak from its normal screening position. The surveyor then identified other viewing angles, and if any of these had different background from the primary viewing direction, the background was noted as a secondary background. During the study, surveyors were free to view the leak location from other angles, such as squatting while viewing the leak or intentionally seeking out a background which was different from those identified by the METEC team.

The fraction of primary and secondary backgrounds for all tests is summarized in Table S-2. The analysis in the main paper utilizes only the primary backgrounds, shown in Table S-3.

Table S-2: Emission Point Primary and Secondary Backgrounds

| Leaking Equipment | Primary and Secondary Backgrounds (fraction of all tests) | | | |
|-------------------|--|----------------|--------|-----|
| | Equip. <1 m | Equip. >1 m | Ground | Sky |
| Ground | - | - | 100% | - |
| Separator | 56% | 0.86% | 27% | 16% |
| Tank | 31% | 9.1% | - | 60% |
| Wellhead | 38% | - | 62% | - |

Table S-3: Emission Point Primary Background

| Leaking Equipment | Primary Background (fraction of all tests) | | | |
|----------------------|---|----------------|--------|------|
| | Equip. <1 m | Equip. >1 m | Ground | Sky |
| Ground | - | - | 100% | - |
| Separator | 63% | - | 16% | 20% |
| Tank | - | - | - | 100% |
| Wellhead | - | - | 100% | - |

S-2.5 Statistical Methods

Bootstrapping was utilized to estimate uncertainty throughout the study. For uncertainty in detection rates, such as the error bars in Figures S-13, S-15 or S-16, the following process was performed:

- Subset the test data into appropriate categories, such as individual bars in Figure S-16.
- For each category, draw 1000 random sets of test records, with replacement (standard bootstrap replicates) and computing the detection rate for replicate.
- Using the Matlab™ `prctile()` function, empirically extract 5% and 95% values for the confidence interval.

For curve fits, such as Figure 2 of the main paper or Figure S-14, uncertainty is represented by a family of curve fits shown as shaded curves behind the nominal curve fit. Each curve fit is calculated by binning the data, computing detection rates for each bin, and then fitting the curve to the detection rates. To bootstrap the points, the following process was performed:

- Subset the test data into appropriate categories, such as compliance or high-experience LDAR surveyors.
- For each category:
 - Create a bootstrap replicate of the data by drawing a random set of test records, with replacement (standard bootstrap methods).
 - Using the binning variable (e.g. wind speed in Figure S-14), bin the data into subsets.
 - Discard any bins with insufficient points.
 - Perform the curve fit. For each plot, linear, semi-log, and log-log curve fits were performed on the data set before bootstrapping and the form with the highest R^2 value was used for the bootstrap fits.
 - Repeat curve fitting for each of 500 replicates

Prior studies (e.g. Ravikumar et al. [1]) utilized logistic regression to represent detection curves. Logistic regression does not produce satisfactory results for this data set because there are too few tests conditions with near-100% detection rates. For example, in Figure 2 of the main paper, emission rates did not go high enough to ‘discover’ the rate at which either compliance and low-experienced LDAR surveyors approached near-100% detection.

S-3 Test Conditions

Tests were conducted at METEC from late January through early November of 2019. Figure S-3 provides an overview of the test activity, including the number of teams at METEC each day, and the number of tests performed each day. A maximum of four camera operators (or teams) were operational on any given day. Generally, teams needed to wait less between testing rounds when three or fewer teams were present. Figure S-4 provides an overview of weather conditions encountered during the testing, and Figure S-5 shows the aggregate daily wind pattern.

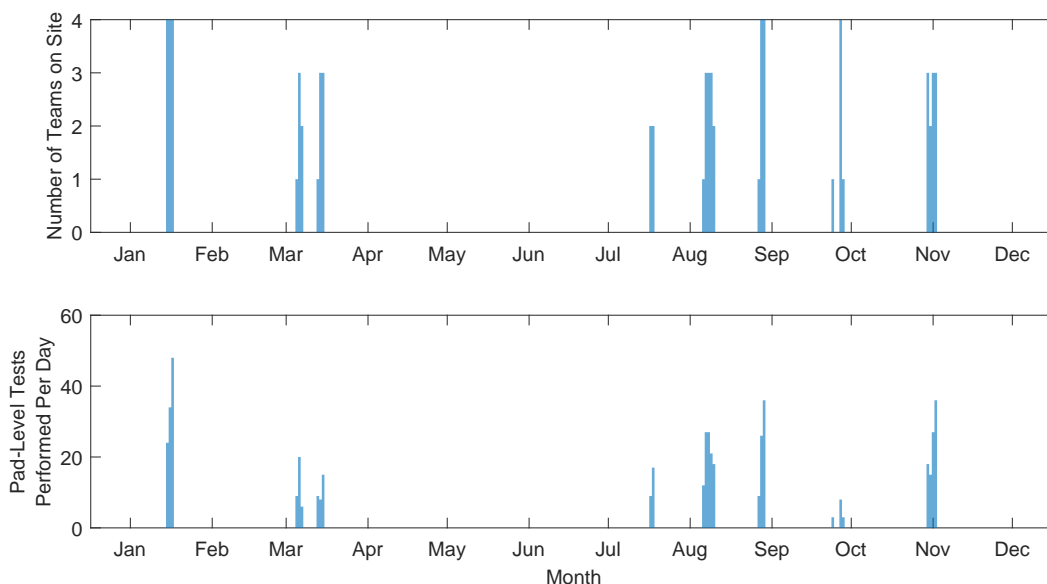


Figure S-3: A calendar view of testing for the entire study. Top panel shows number of teams who were on site on each test day. Bottom panel indicates the number of tests performed on each test day.

Histograms of emission rates are shown in Figure S-7. Emission rates were chosen to be representative of rates seen in field studies for similar components [2, 3].

All test points utilized for the study are listed in Table S-4. Data included in the table matches the METEC emission point ID with qualitative data regarding the most likely viewpoints when identifying emissions from the emissions point.

To avoid ‘tipping off’ surveyors, most tests were conducted utilizing industrial methane, which is unodorized and has heavier hydrocarbons in trace amounts. However some testing conducted earlier in the study utilized market gas taken from the nearby distribution system. This gas was odorized (i.e. had mercaptans added), and on average was 0.86 methane (mass fraction), with the

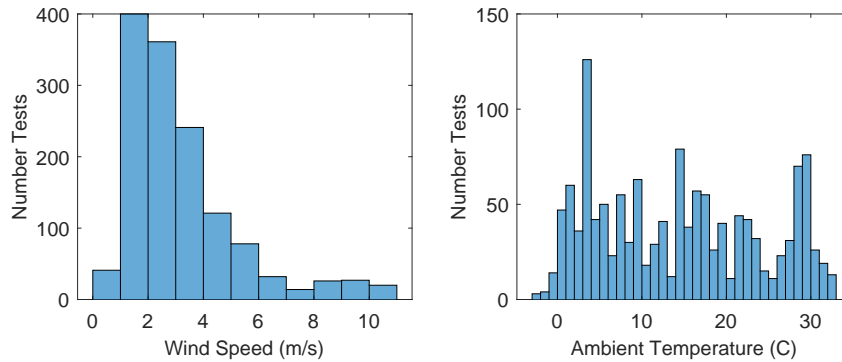


Figure S-4: Weather conditions encountered during testing. Left panel provides a histogram of wind speeds, measured on site at a height of approximately 5 meters. Right panel provides a histogram of ambient temperatures for each test. A *test* is defined as a single camera operator (or team) screening a combination of one leak point on one pad.

balance being predominantly ethane. In total, 60 pad-level test configurations used only odorized gas and 33 used a combination of odorized market gas and methane at different leak points, while 319 used methane only; 3.7% of test configs utilized some amount of odorized gas.

Since the odorized gas was utilized early in the testing, and most compliance teams tested early in the testing, a larger fraction of compliance teams tested using odorized natural gas: 49% of compliance team reports used odorized gas, compared to 3.7% of LDAR team reports.

The *primary detection background* is the background of the camera’s view, behind the leak location, when viewed from the most typical, convenient location to screen for a leak. The *secondary detection background* has the same definition, but represents a viewing angle which an operator *may* use to screen the component. The values in these two fields are:

Sky The leak point would normally be viewed against the sky.

Ground The leak location is below a typical camera height, and the background behind the leak location is some view of the ground - either gravel or grass.

Equip < 1 m Camera background is primarily another piece of equipment that is less than one meter away.

Equip > 1 m Camera background is primarily another piece of equipment that is more than one meter away.

Exposure indicates whether the leak point is inside an enclosure. For this study, all ‘inside’ points were inside the doors of the enclosure at one end of a horizontal separator, commonly called a ‘dog house.’

Viewing Angle indicates the cardinal bearing, in degrees, of the primary viewing angle for the leak point, where north is 0°.

Used in Test lists the test IDs where each leak point was used.

Figure S-8 shows the overall detection rate seen for each emission point, coded by the type of

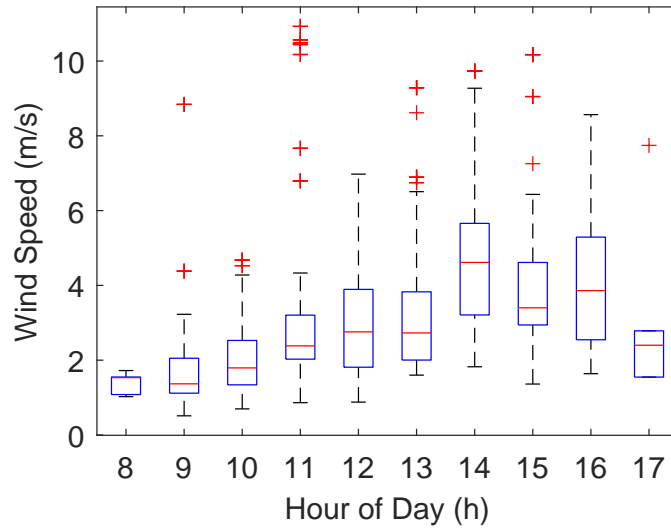


Figure S-5: While highly variable overall, wind speeds at METEC follow a relatively predictable pattern on a daily basis, with lower winds in early morning giving way to higher winds during mid-day.

equipment on which it is located. Note that the bars on this chart show the full range of emissions released in any test for each point. One leak point, $4W - 01$, was the only underground emission point utilized in the test, and was found by none of the operators. In contrast, one leak point, $3T - 22$, was found by all operators.

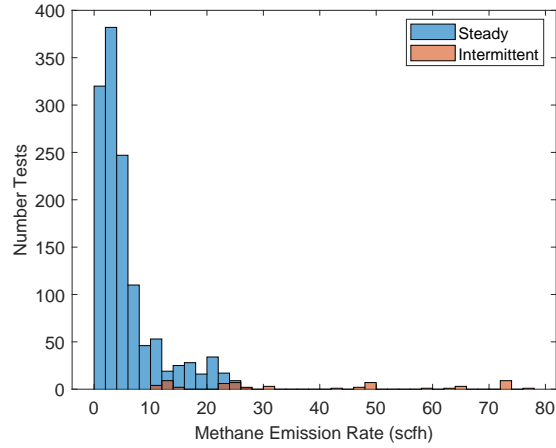


Figure S-6: Distribution of emission rates used during testing. Most tests utilized steady emission rates. Average emission rates for intermittent emission points are indicated, but are not utilized in most analysis.

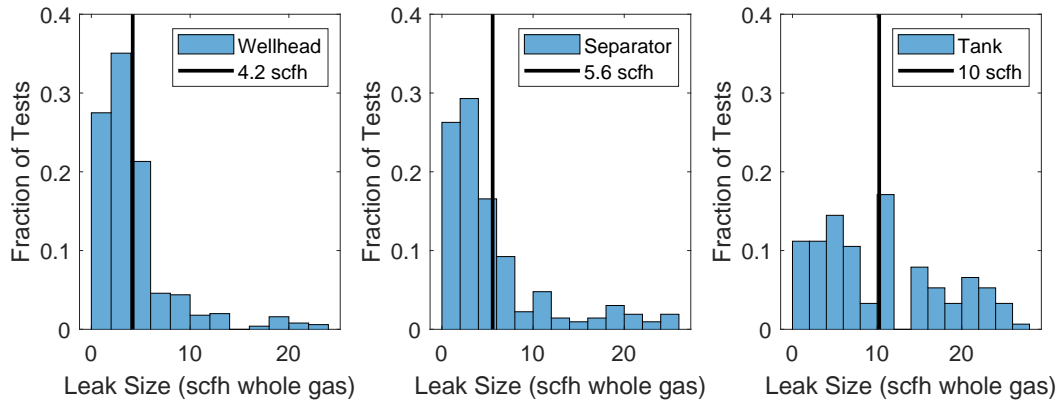


Figure S-7: Emission rates by equipment types. Chosen emission rates are representative of data collected in field studies. Intermittent emitters are excluded. Mean separator and wellhead emission rates are similar, as are the distributions, while emission rates from tanks are larger.

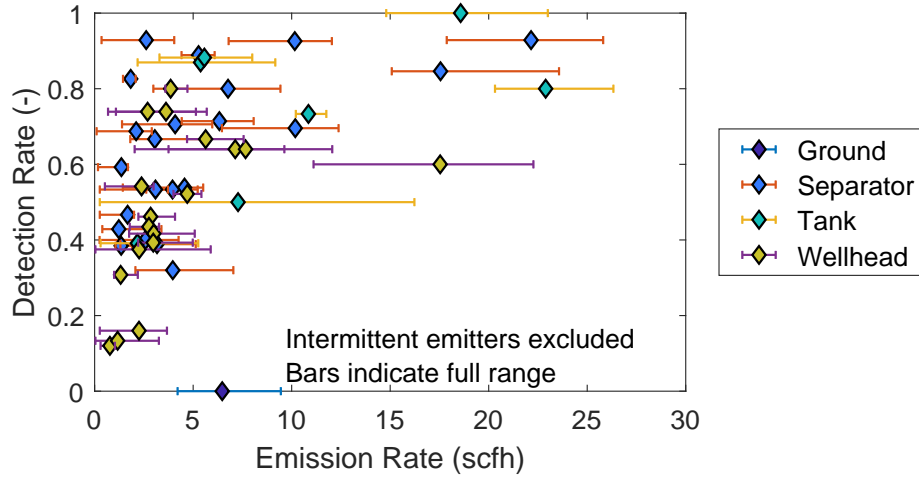


Figure S-8: Detection rate as a function of emission rate for all test points. Point color indicates the type of equipment where the emission point is located. Horizontal error bars indicate the full range of emissions released *across all tests performed* from each test point. Each point indicates a combination of an emission location and a test id.

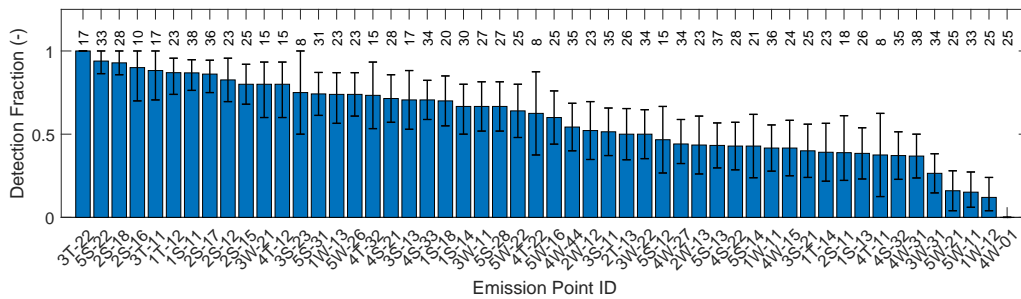


Figure S-9: Detection rate for each emission point used in the study. Bars indicate the observed detection rate for each emission point, by METEC emission point ID. Error bars indicate 90% bootstrap confidence intervals on the detection rate for each point. Numbers above bars indicate the number of tests performed on each test point.

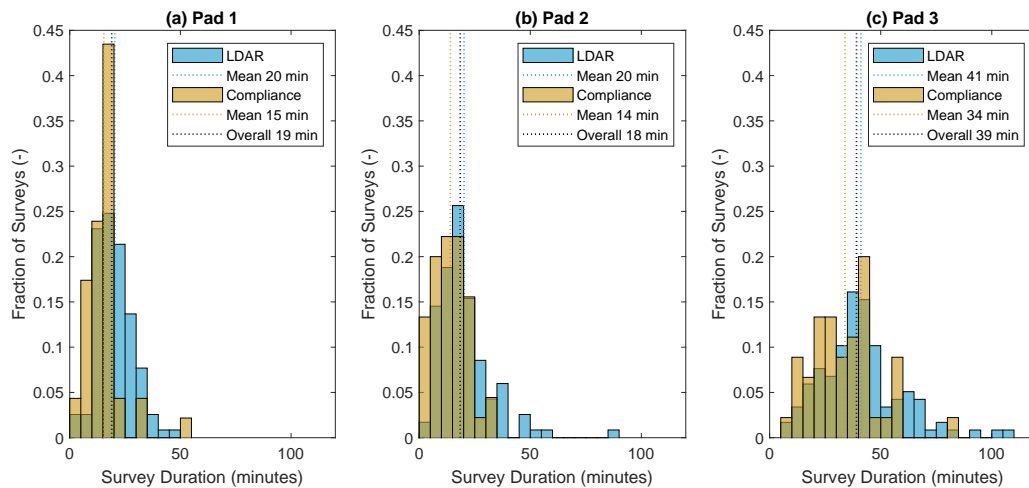


Figure S-10: Time spent on surveys by all surveyors, segregated by pad. Histograms are clipped to 120 minutes. Surveys on pads 1 and 2 exhibit similar survey times (Mean: 19 minutes, range: 3 to 52 minutes for Pad 1 and Mean: 18 minutes, range: 1 to 89 minutes for Pad 2), while survey times on Pad 3 are substantially longer – Mean: 39 minutes, range: 9 to 108 minutes – and exhibit more variation. (90% central confidence intervals.)

Table S-4: Emission Point Characteristics

| METEC Point ID | Study Pad ID | Primary Detection Background | Secondary Detection Background | Exposure | Unobstructed Viewing Angle | Used in Test Configurations (ID) |
|----------------|--------------|------------------------------|--------------------------------|----------|----------------------------|----------------------------------|
| 1S – 11 | P1 | Equip (<1 m) | - | Inside | 270 | 2,7 |
| 1S – 13 | P1 | Sky | - | Outside | 360 | 6 |
| 1S – 14 | P1 | Sky | - | Outside | 360 | 1,4,8 |
| 1S – 18 | P1 | Equip (<1 m) | Ground | Outside | 300 | 1,8 |
| 1T – 12 | P1 | Sky | Equip (>1 m) | Outside | 270 | 5 |
| 1T – 14 | P1 | Sky | - | Outside | 360 | 5 |
| 1W – 11 | P1 | Ground | Ground | Outside | 360 | 6,7 |
| 1W – 12 | P1 | Ground | Ground | Outside | 360 | 1 |
| 1W – 13 | P1 | Ground | Ground | Outside | 360 | 5 |
| 2S – 11 | P1 | Equip (<1 m) | Ground | Outside | 270 | 4 |
| 2S – 12 | P1 | Equip (<1 m) | Ground | Outside | 270 | 5 |
| 2S – 15 | P1 | Equip (<1 m) | Ground | Outside | 300 | 1 |
| 2S – 16 | P1 | Equip (<1 m) | Ground | Outside | 270 | 7 |
| 2S – 17 | P1 | Equip (<1 m) | Ground | Outside | 270 | 6,8 |
| 2S – 18 | P1 | Sky | - | Outside | 360 | 2 |
| 2T – 13 | P1 | Sky | - | Outside | 360 | 6 |
| 2W – 12 | P1 | Ground | - | Outside | 360 | 5 |
| 2W – 13 | P1 | Ground | Equip (<1 m) | Outside | 360 | 5 |
| 3S – 11 | P2 | Ground | Equip (<1 m) | Outside | 300 | 2,9 |
| 3S – 13 | P2 | Sky | - | Outside | 360 | 4 |
| 3S – 21 | P2 | Ground | Equip (<1 m) | Outside | 180 | 3,8 |
| 3S – 23 | P2 | Ground | Equip (>1 m) | Outside | 360 | 9 |
| 3T – 11 | P2 | Sky | Equip (<1 m) | Outside | 360 | 4 |
| 3T – 22 | P2 | Sky | Equip (<1 m) | Outside | 360 | 4 |
| 3W – 11 | P2 | Ground | Equip (<1 m) | Outside | 180 | 2 |
| 3W – 21 | P2 | Ground | Equip (<1 m) | Outside | 360 | 3 |
| 3W – 22 | P2 | Ground | Equip (<1 m) | Outside | 360 | 5,8 |
| 3W – 31 | P2 | Ground | Equip (<1 m) | Outside | 360 | 6,9 |
| 4S – 21 | P3 | Equip (<1 m) | - | Inside | 270 | 2 |
| 4S – 22 | P3 | Equip (<1 m) | - | Inside | 270 | 2 |
| 4S – 32 | P3 | Ground | Equip (<1 m) | Outside | 360 | 6,8 |
| 4S – 33 | P3 | Equip (<1 m) | - | Inside | 270 | 5,8 |
| 4T – 11 | P3 | Sky | Equip (<1 m) | Outside | 360 | 9 |
| 4T – 12 | P3 | Sky | Equip (<1 m) | Outside | 360 | 3 |
| 4T – 22 | P3 | Sky | Equip (<1 m) | Outside | 360 | 9 |
| 4T – 32 | P3 | Sky | Equip (<1 m) | Outside | 360 | 3 |
| 4W – 01 | P3 | Ground | - | Outside | 360 | 6 |
| 4W – 15 | P3 | Ground | Equip (<1 m) | Outside | 360 | 5 |
| 4W – 27 | P3 | Ground | - | Outside | 360 | 5,7 |
| 4W – 31 | P3 | Ground | Equip (<1 m) | Outside | 360 | 2,7 |
| 4W – 44 | P3 | Ground | Equip (<1 m) | Outside | 360 | 1,8 |
| 5S – 12 | P3 | Equip (<1 m) | Sky | Outside | 270 | 5,9 |
| 5S – 13 | P3 | Equip (<1 m) | - | Outside | 300 | 1,7,9 |
| 5S – 14 | P3 | Equip (<1 m) | - | Outside | 300 | 3,7 |
| 5S – 22 | P3 | Equip (<1 m) | - | Outside | 270 | 2,8 |
| 5S – 28 | P3 | Sky | - | Outside | 270 | 5,8 |
| 5S – 31 | P3 | Equip (<1 m) | - | Outside | 300 | 3,5,9 |
| 5W – 11 | P3 | Ground | Equip (<1 m) | Outside | 360 | 1,9 |
| 5W – 16 | P3 | Ground | Equip (<1 m) | Outside | 360 | 6 |
| 5W – 21 | P3 | Ground | Equip (<1 m) | Outside | 360 | 3,7 |
| 5W – 22 | P3 | Ground | Equip (<1 m) | Outside | 360 | 6 |
| 5W – 26 | P3 | Ground | Equip (<1 m) | Outside | 360 | 5 |

S-4 Detection Curves and Comparison to Ravikumar et al.

The main paper compares 90% detection probabilities to Ravikumar et al.[1]. The focus of the Ravikumar study was somewhat different than the current study. All data was taken during a single week, in relatively constant environmental conditions. The optical gas imaging (OGI) camera was tripod-mounted for all imaging. After data collection, the visibility of plumes in each video was assessed by expert observers, and a detection probability was extracted from the resulting set of detections. Ravikumar proposes a 90% probability-of-detection curve of the form $r = 1.845d^{1.975}$ where r is the emission rate that produces at 90% probability of detection at a distance of d meters. For the mean detection distance reported in this study (2.7 m (8.9 ft)), the Ravikumar equation produces 90% probability-of-detection at an emission rate of 13 g/h (0.7 scfh).

In contrast to the Ravikumar study, which used logistic regressions to develop detection curves, logistic regression could not be utilized in this study because there were too few samples with near-100% detection rates – i.e. conditions such as surveyor experience and environmental conditions did not produce a sufficient TP and TN reports for the logistic regression to identify a $\approx 100\%$ detection probability for key independent variables. Therefore, this study utilizes linear or log-log detection probability curves.

To compare the Ravikumar results to detection curves developed here a 90% probability-of-detection was calculated for several key independent variables. The data were bootstrapped, and a probability-of-detection curve was fitted to each bootstrap replicate. The 90% probability-of-detection was then calculated from the bootstrap family of detection curves. These data were utilized to calculate a central estimate – from the non-bootstrap curve fit – and a confidence interval from the bootstrap curve fits. Results are summarized in Table S-5 for wind speed (linear fit) and emission rate (log-log fit).

Table S-5: 90% Probability-of-Detection Rates

| Affiliation | Prior Sites Surveyed | Emission Rate (scfh) | Emission Rate (slpm) | Wind Speed (m/s) |
|-------------|----------------------|----------------------|----------------------|-----------------------|
| Compliance | 12 - 550 | 27.7 [8 to 42.4] | 13 [3.76 to 20] | -2.78 [-4.53 to 27.4] |
| LDAR | 25 - 200 | 83.1 [18.4 to 163] | 39.1 [8.67 to 76.7] | -16 [-4.63 to 30.4] |
| LDAR | 700 - 4000 | 7 [5.52 to 16.4] | 3.29 [2.6 to 7.7] | -1.37 [-3.63 to 18.9] |

* Negative values indicate that 90% probability of detection is not achieved at any wind speed using the curve fit applied in this analysis, see Figure S-14.

S-5 Experience Analysis

Surveyors self-reported the number of facilities they had previously surveyed prior to the study, and this variable proved to be one of the best predictors of overall detection rate, see Figure S-11. These values are doubtlessly approximate, as few surveyors keep a comprehensive log of their prior work. However, these data appear representative of the hands-on experience of the surveyor. Assuming an average of 4 sites/day and a 200-day working year, 4000 site surveys represents five years of

full-time survey work.

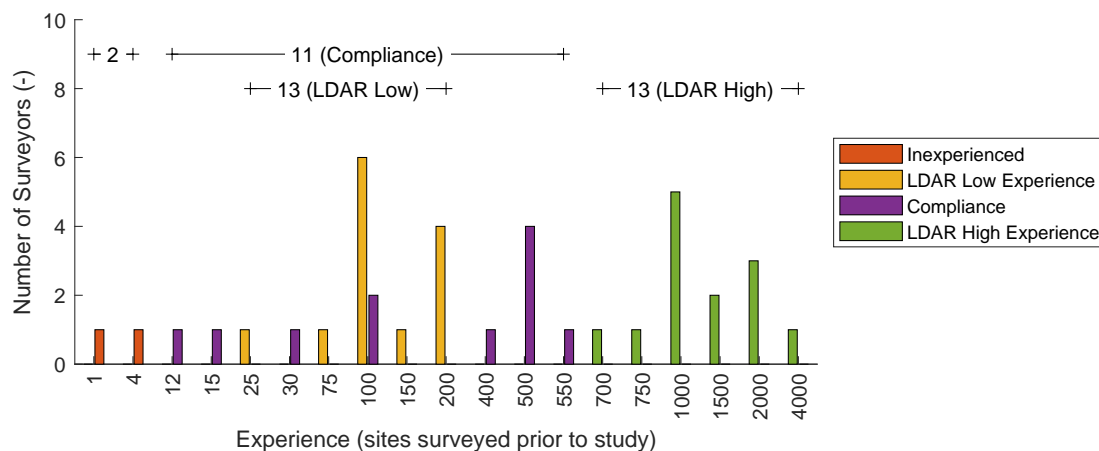


Figure S-11: Surveyor experience. Each bar represents the count of surveyors who self-reported the indicated number of sites surveyed prior to the study. Colors indicate groupings utilized for the study. Lines above bars indicate the total number of surveyors in each grouping. Surveyors with <10 sites (surveyors WV1 and QO1) were considered ‘inexperienced’ and are not included in most charts. Remaining surveyors are divided into two approximately equal groups.

To analyze the impact of experience, thresholds were selected to group surveyors’ performance by ‘the number of sites surveyed before testing’. Two thresholds were selected – the number of sites required to be ‘experienced’ (551), and the minimum number of sites to be considered ‘trained’ (10). The latter threshold was selected to remove 2 participating compliance surveyors (WV1 and QO1) who had essentially no experience prior to the study. Additionally, the LDAR group had more surveyors with higher experience than compliance group, and there was a large gap between a group of LDAR surveyors with lower experience (25 - 200 sites), and those with higher experience (≥ 700 sites) – see Table S-7 as well. Applying the thresholds, which combined all compliance surveyors with some experience into a single group, created three subgroups with similar numbers of surveyors: 13 low-experience (25 - 200 sites) and 13 high-experience (700 - 4000 sites) LDAR surveyors and a single group containing all 11 compliance surveyors (12 - 550 sites) with some experience. Table S-6 summarizes these groupings.

Table S-6: Fraction of Reports by Affiliation and Experience

| Experience Group | Nominal Experience Range | Experience Range in Data | Total Tests | Fraction of Tests |
|------------------|--------------------------|--------------------------|-------------|-------------------|
| LDAR Low | 10 to 551 | 25 to 200 | 478 | 0.34 |
| LDAR High | 551 to 4001 | 700 to 4000 | 530 | 0.38 |
| Compliance | 10 to 4001 | 12 to 550 | 296 | 0.21 |
| Inexperienced | 0 to 10 | 1 to 4 | 104 | 0.074 |

Detection rates for individual surveyors is shown in Figure S-12 for surveyors who completed at least 15 non-zero emission tests – i.e. test on which a detection rate could be calculated. Differences

in detection rate for each group are apparent ... but the figure also illustrates that the range of detection rates in each group is large.

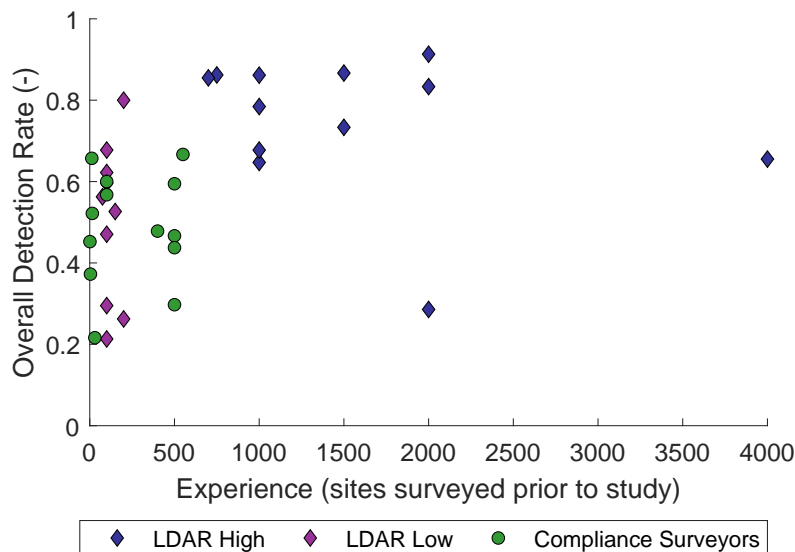


Figure S-12: Detection rate for individual surveyors. An individual point is shown for each surveyor who completed at least 15 non-zero emission tests, divided into the groups used for the study. These points are shown as outlines in the background of Figure 1 in the main paper. While there are outliers in all groups, on average LDAR surveyors with high experience levels have higher detection rates than the other two groups.

Figure S-13 illustrates the variability of detection rate for each group, and compares between the groups.

Two analyses were performed to further illustrate the validity of this grouping. First, test data was ordered by increasing experience of the surveyor and grouped into bins that had a minimum of 100 non-zero emission tests. The detection rate was then calculated for each bin. Results from this analysis is shown in Table S-7, and in Figure 1 in the main paper. Results show a significant increase in detection rate for surveyors with more than 551 surveys completed prior to the study, although there are exceptions for individual surveyors, i.e. high-experienced surveyors with low detection rates and low-experienced surveyors with high detection rates, as shown in Figure S-12.

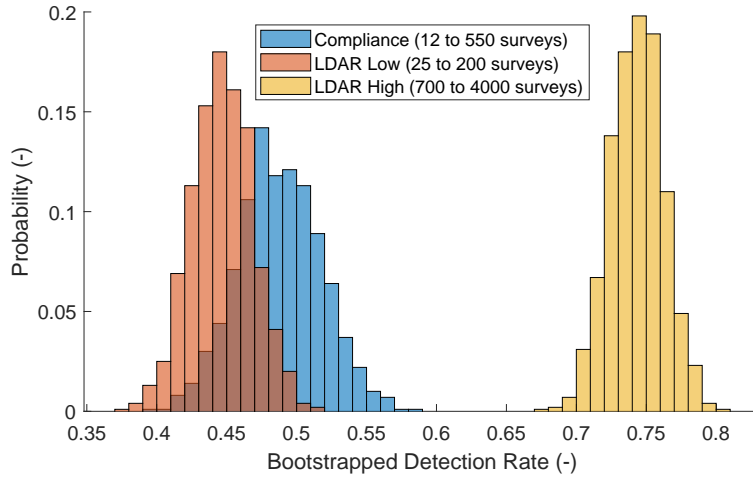


Figure S-13: Detection rate histograms for experience groupings. Histograms illustrate 1000 bootstrapped replicates of detection rate for each experience grouping utilized in the study. Overlap in the histograms for compliance and low-experience LDAR is shown with shading. Compliance surveyors and LDAR surveyors with low experience exhibited similar detection rates over all tests, and bootstrap uncertainty in detection rates, while LDAR surveyors with high experience exhibited significantly higher detection rates overall.

Table S-7: Groupings for Experience Cutoff Sensitivity Analysis

| Group ID | Surveys Conducted | | Surveyor Type | Total Tests | Detection Rate |
|----------|-------------------|---------|---------------|-------------|---------------------|
| | Minimum | Maximum | | | |
| 1 | 1 | 12 | Compliance | 128 | 0.48 [0.4 to 0.55] |
| 2 | 15 | 75 | Both | 101 | 0.41 [0.32 to 0.49] |
| 3 | 100 | 100 | Both | 353 | 0.47 [0.42 to 0.51] |
| 4 | 150 | 200 | LDAR | 125 | 0.42 [0.35 to 0.5] |
| 5 | 400 | 500 | Compliance | 128 | 0.45 [0.38 to 0.53] |
| 6 | 550 | 750 | Both | 106 | 0.83 [0.76 to 0.89] |
| 7 | 1000 | 1000 | LDAR | 243 | 0.74 [0.7 to 0.79] |
| 8 | 1500 | 4000 | LDAR | 181 | 0.69 [0.63 to 0.74] |

A second analysis computed overall detection rate (true positives divided by true positives + false negatives) across a range of experience cutoffs while requiring a minimum of 100 reports in each experience bin. The cutoff between inexperienced and low experience was varied between 0 and 100 sites, while the cutoff between low and high experience was varied between 200 and 600 sites. Across all valid combinations of these ranges, the detection rate varied by no more than 5.8 percentage points – -3.8 to +0.32 percentage points for low experience and -5.8 to +0 percentage points for high experience.

Key figures are included in the main paper. Three additional figures, detection curves for wind speed (Figure S-14), time-of-day by experience (Figure S-15) and equipment type by experience (Figure S-16) are included below. Variables which were controlled are noted in each figure caption.

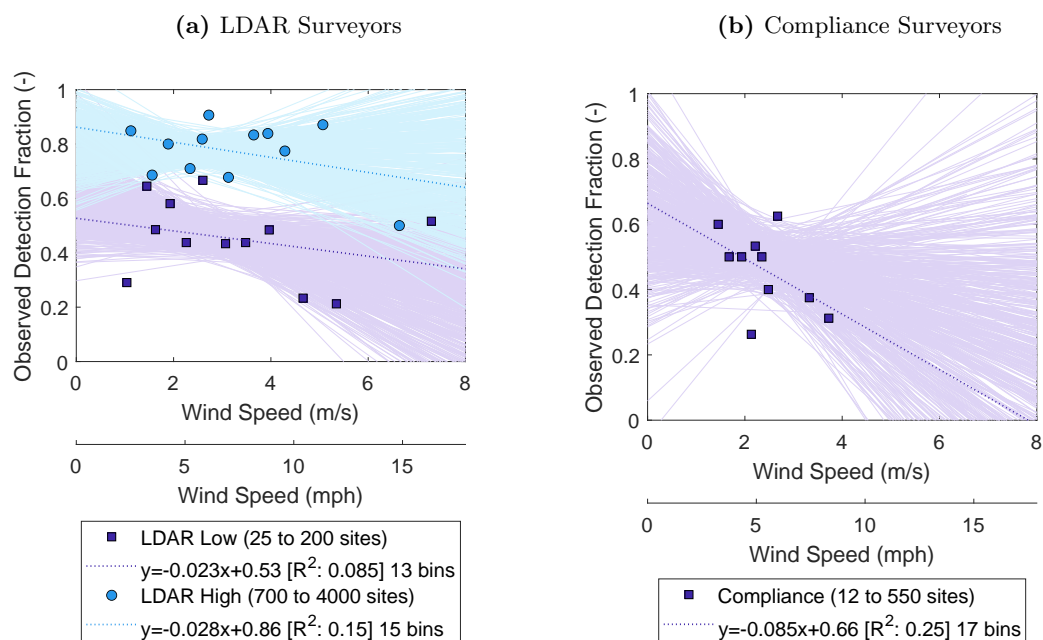


Figure S-14: Detection rate by experience and wind speed. Wind speed is known to have a significant impact on OGI detections; higher wind speeds disperse emissions and make detection more difficult. Detection curves based upon wind speed have lower R^2 values than those based on emission rate (see main paper), but show a similar impact of experience. Plots are restricted to winds 0-9 m/s, and ambient temperature 0-35 C, and exclude tests without emissions and all intermittent emitters; 30 samples per bin for panel (a), 15 for panel (b).

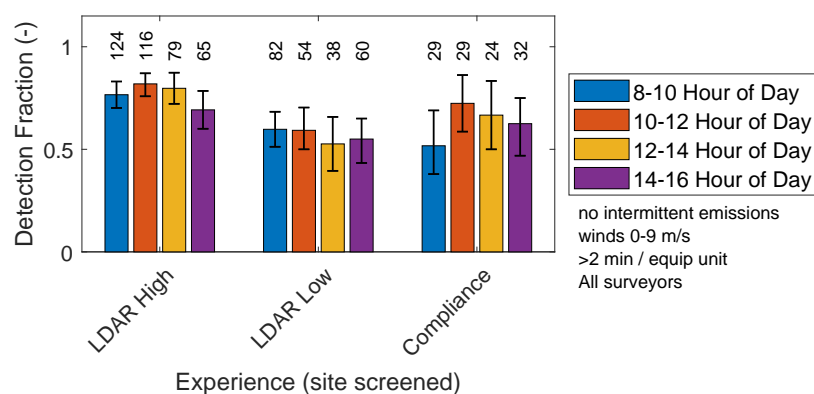


Figure S-15: Detection rate for non-zero emission points by hour of the day. There is a statistically insignificant decrease in detection fraction in afternoon hours for both experience groups. However, the relationship is weak ($R^2 \leq 0.35$) and since the wind is also higher in the afternoon (Figure S-5), the time-of-day is likely not a good predictive variable. Data is controlled for both wind speed and time spent on surveys.

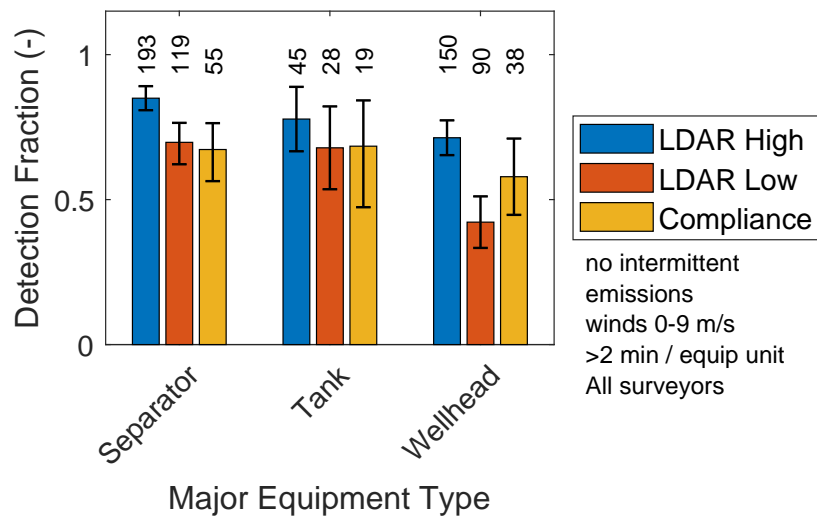


Figure S-16: Detection rate by equipment type and experience. For separators, the most experienced surveyors have detection rates that are significantly higher than either less experienced LDAR surveyors or compliance surveyors – the enclosed components on separators may contribute to the differences. For wellheads, experienced surveyors are significantly better than less-experienced LDAR surveyors, but only qualitatively better than compliance surveyors. Ground backgrounds are common for wellhead components, and, as noted in the main paper, ground backgrounds tend to be more challenging than either equipment or sky backgrounds. The greater viewing distance specified in compliance protocols, which diversifies wellhead backgrounds, may contribute to the better performance of compliance surveyors. The difference between experience levels is not significant for tanks, where emissions are most often viewed against sky or equipment backgrounds. Data is controlled for wind speed and time spent on surveys.

S-6 Affiliation Analysis

Surveyor affiliation also has an impact on the detection rate. As indicated in the surveyor meta-data comments, compliance surveyors, as a group, tend to use a different protocol than LDAR surveyors, as a group, although protocols vary within both groups. These differences are largely driven by the purpose of the surveys performed by each affiliation. Protocols for compliance surveys are targeted at gross violations of cognizant regulations, and therefore favor moving quickly through many facilities while looking for substantial emission rates. Many compliance protocols do not allow surveyors to open equipment, climb on tank catwalks or, in some cases, step inside the liquid containment berm around equipment. In contrast, LDAR protocols generally attempt to find all leaks, no matter how small, and no matter what location. LDAR surveyors are generally empowered to open cabinets, climb stairways, and otherwise get close to equipment. A portion of the detection rate differences for these two groups may be due to this type of protocol difference.

Figure S-17 shows the surveyor-reported distance between the camera and leak at the time of detection. While LDAR surveyors were somewhat closer during detection – a mean distance of 8.6 ft versus 9.7 ft for compliance surveyors – the distance histogram is substantially overlapped. Therefore, protocol differences have only a small impact on the *distance* between surveyor and potentially leaking equipment, but access to internal compartments and catwalks could have a substantial impact on how these two types of surveyors perform surveys.

Figure S-18 compares detection rates, by affiliation and hour-of-day. This plot is analogous to Figure S-15 for experience levels. Figure S-19 illustrates differences in detection rate by type of major equipment.

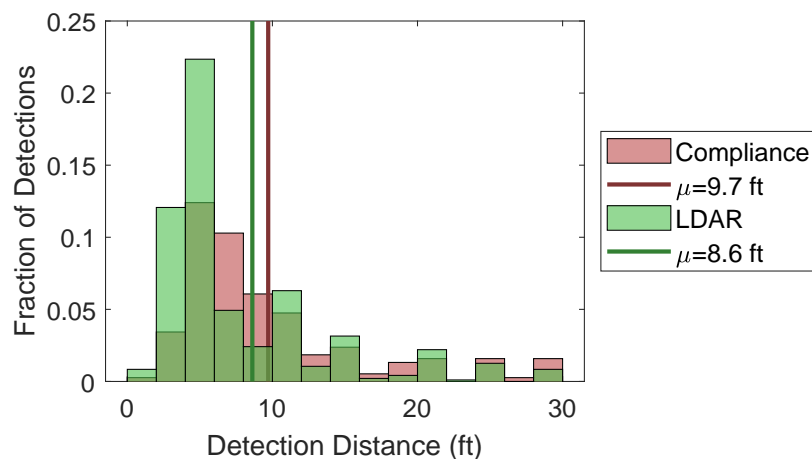


Figure S-17: Detection distance for compliance and LDAR surveyors. LDAR surveyors are somewhat closer to leaks at time of detection, but the distribution of detection distances of the two types of surveyors is heavily overlapped. Mean detection distance across all reports is 2.7 m (8.9 ft).

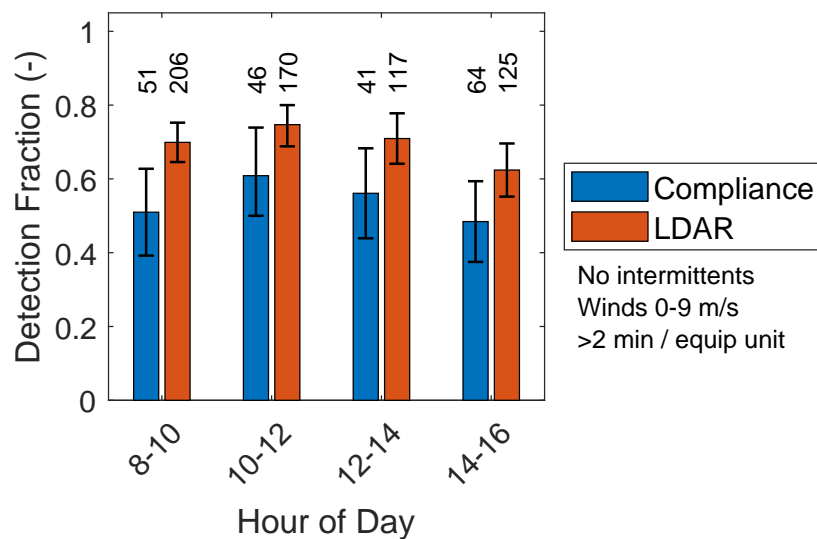


Figure S-18: A comparison of detection rates by affiliation type, segregated by hour-of-day. Detection rate for compliance surveyors are lower than those for LDAR surveyors, driven, at least in part, by differences in protocols between the two types of surveyors. In the mean, detection rates generally rise from early morning to near mid-day, and drop toward late afternoon, although uncertainty is high enough that trends may not be statistically significant. The increase in early morning may be due to increased familiarity with the test site and the challenging nature of the test. Both fatigue and increased wind speed after noon (see Figure S-5) may be factors contributing to a lower detection rate in late afternoon.

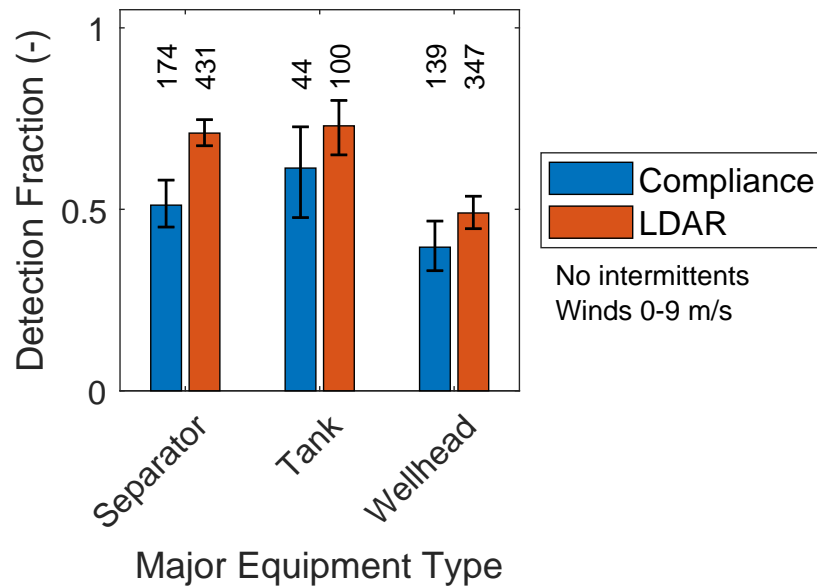


Figure S-19: Detection rate by equipment type by affiliation. For tanks and wellheads, detection rates for compliance and LDAR surveyors have similar ratios to the overall ratio in detection rates for these two affiliations. However, for separators, the detection rate for compliance surveyors is lower than LDAR surveyors. Separators are also the only major equipment category where some emission points were in an enclosed space – the cabinet (‘doghouse’) attached to the separator. Since many compliance survey protocols do not allow surveyors to open enclosed equipment, small leaks inside the separator enclosure were difficult to detect, possibly leading to a lower detection rate.

S-7 Other Variables

Independent variables which were reasonably strong predictors of detection rates are discussed in the main paper; this section provides plots for other variables of interest. Figure S-20 illustrates that wind speed impacted detection rates similarly for all emission rates. Figure S-21 shows how inspection times changed with temperature. Figure S-22 summarizes total emissions found across all non-zero emissions tests (referenced in the ‘Guidance’ section of the main paper).

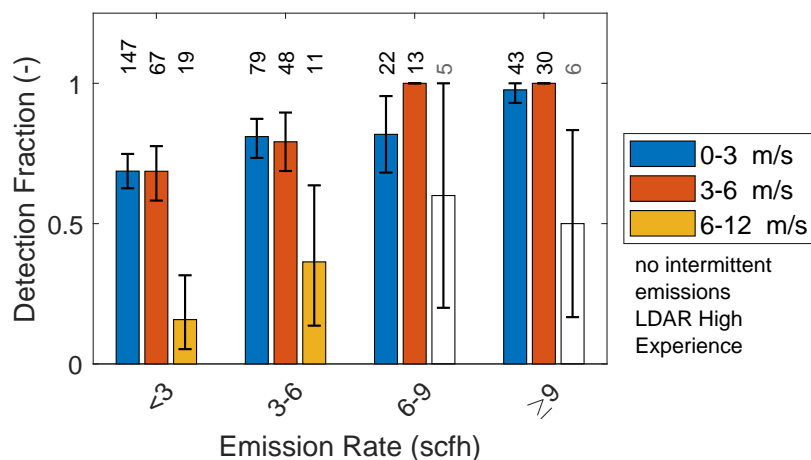
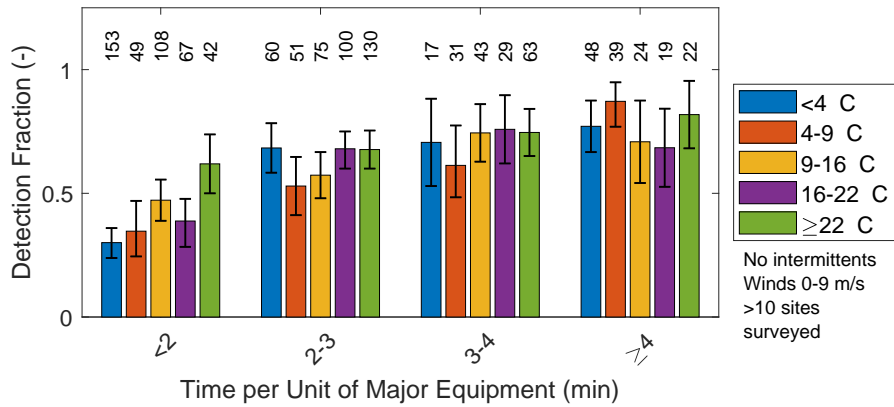
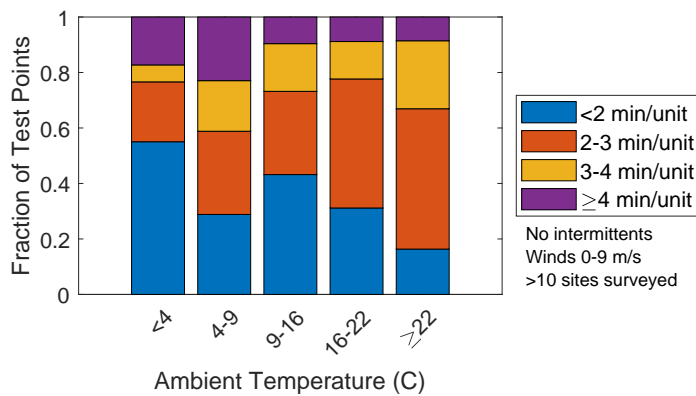


Figure S-20: Impact of the emission rate and wind speed on detection rates. Data is controlled to only consider results from highly experienced LDAR surveyors who had screened 700 or more facilities prior to the study. For all emission sizes, detection rates drop off dramatically with wind speed above 6 m/s, coupled with much larger uncertainty. Below 6 m/s, there is no statistical difference in detection rate for all leak sizes. These data indicate that a wind speed cutoff for surveys may need to be set to 6 m/s, however, since the majority of testing occurred at ≤ 6 m/s, and specifically there were few points with emission rates >6 scfh and wind >6 m/s, no definitive statements can be made.



(a) Detection rate by time spent on each unit of major equipment, by ambient temperature.



(b) Survey time choices by ambient temperature

Figure S-21: Time spent inspecting by ambient temperature. Time data is normalized to major equipment units, where a major equipment unit is a well head, tank, or separator. Data is binned by temperature to divide data into roughly equal reports per bin. Surveyors showed a tendency to scan more equipment for less than 2 minutes or more than four minutes at cold temperatures – fully 55% of surveys done at <4 °C and 29% done 4-9 °C were completed at an average speed of <2 minutes per unit of major equipment. Despite shifts in survey time, mean survey times are similar for all temperatures: 2.3 to 3.1 minutes per unit of major equipment. Since short survey times are predictive of poorer detection rates, surveying more units at faster speeds in cold temperatures tends to decrease detection rates, but the impact is most evident for the smallest emission rates.

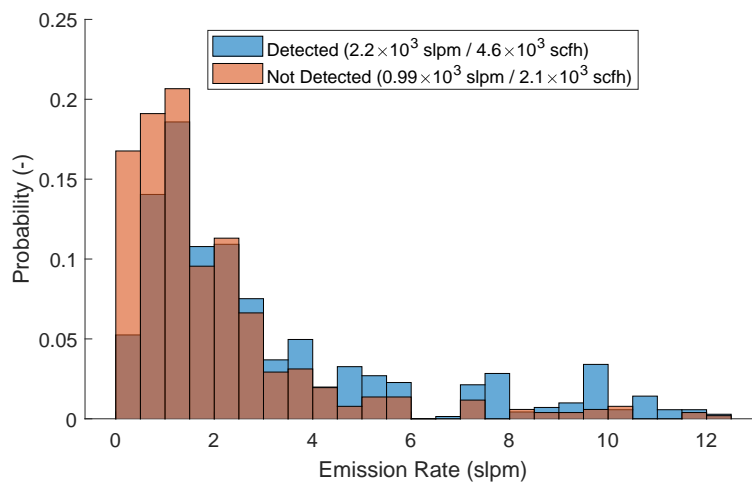


Figure S-22: Summary of detected emissions. Overlaid histograms show the distribution of emission detected (true positives) and not detected (false negatives) for the testing performed in this study. While emission rates were skewed to the low end of emission rates, relative to studies of well pad emissions, surveyors detected 69% of emissions, due to the higher detection rates for larger emitters. Figure includes all non-zero emission tests and omits intermittent emitters and tests performed by surveyors who had performed less than 10 surveys prior to the study.

S-8 Videos

Included in the supplementary information are 5 videos which provide specific side-by-side examples of observation conditions where viewing angle, background, or contrast made a substantial difference in the effective method detection limit (EMDL) of the OGI survey. This section paraphrases the caption of each video to help the reader identify the content of the video.

S-8.1 SI Video 1: OGI observations of detected OEL leak under different conditions using auto and HSM modes

- *Panel a:* 3.92 scfh emissive plume under cloudy, cold, conditions (45.7 °F, wind speed 2 m/s, 1/30/18 9:05 am).
- *Panel b:* 3.63 scfh absorptive plume under partly sunny, mild conditions (70.2 °F, wind speed 3.6 m/s, 8/20/18 2:18 pm).
- *Description:* In panel (a), the plume is primarily detected against the cold ground surface (overnight ambient temperature of 28 °F), as opposed to the proximate background of the emitting component, since the gas temperature, and effective temperature of the component, are similar at the time of observation [33.8 °F, only available in (a)]. Due to wind direction, the only detection opportunity in (b) is against the ground, with direct solar incident radiation creating additional image noise in the HSM mode compared to (a). As conditions change and the ΔT between the gas and individual background approach zero, EMDL increases, making surveyor experience and training for optimal positioning to preferred backgrounds more important. In addition, the opportunity for expert positioning is limited for near-ground emission points.

S-8.2 SI Video 2: Observations of detected connector leak under different conditions using HSM mode.

- *Panel (a):* 3.21 scfh emission under partly cloudy skies (85.0 °F, wind speed 2.6 m/s, 9/11/18 12:11 pm).
- *Panel (b):* 6.86 scfh emission under clear skies (76.4 °F, wind speed 1.3 m/s, 9/12/18 9:31 am)
- *Description:* Videos shown were produced by the same surveyor and camera. In (a), the lower emission rate is detectable against the ground and therefore can be identified from a wider range of observation positions. In (b), the emission is 2 times the emission rate and shown in one half the wind speed, and is only detectable against the proximate background of the emitting component (likely due to low gas/ground temperature delta). Case (b) can be detected only in specific wind conditions and observation positions that create this background overlap state, greatly reducing the detection probability.

S-8.3 SI Video 3: Observations of detected flange leak using different backgrounds.

- *Panel (a)*: 3.68 scfh emission against a sky background (70.7 °F, wind speed 4.0 m/s, 8/20/18 2:44 pm).
- *Panel (b)*: 4.0 scfh emission under partly cloudy skies with proximate tank background (67.1 °F, wind speed 1.8 m/s, 8/21/18 1:00 pm)
- *Description*: In (a), the emission is difficult to detect in auto mode, but more visible in HSM mode (differential processing assisted by uniform sky background). The flange is connected to a tank just off-screen in (a) that is partially blocking the wind in this case, lowering dispersion and enhancing detection capability. In (b), under a different wind direction, the surveyor used the uniform and higher contrast tank surface (i.e. higher ΔT relative to the gas emission) as a background to enhance detection capability. In (b), the full video shows the surveyor repositioning several times around the component under inspection to establish a near-optimal viewing direction and background.

S-8.4 SI Video 4: Observations of detected separator level controller leak under similar overcast conditions from three different observation positions.

- *Panel (a)*: 2.17 scfh emission with near optimal background positioning (64.4 °F, wind speed 3.67 m/s, 8/20/18 11:49 am).
- *Panel (b)*: 2.16 scfh emission with non-optimal distant background (57.7 °F, wind speed 3.1 m/s, 8/21/18 9:06 am)
- *Panel (c)*: 2.16 scfh emission with non-optimal high variance (i.e. high contrast) background (59.4 °F, wind speed 2.7 m/s, 8/21/18 12:06 pm)
- *Description*: The component is housed in an enclosure attached to one end a separator (commonly called a ‘doghouse’) with doors on three sides, and the separator tank on the fourth side (see Figure S-23). In (a) one or both side doors are left closed, partially shielding the wind and the detection is made against proximate, uniform, and favorable ΔT background formed by the shed wall. This illustrates that the surveyor was seeking an optimal background condition. In (b), the surveyor opened both shed doors, creating a higher wind sweep of the emission, resulting in higher plume dispersion, and forcing a more difficult detection against the distant ground in the background. In (c), the surveyor is located close to the component under inspection, but is non-optimally positioned in the shed doorway, creating larger than necessary background temperature range that may stretch the intensity scale of the camera and complicate detection – i.e. it likely reduced EMDL.

S-8.5 SI Video 5: Observations of detected leak illustrating method interference in HSM mode.

- *Panel (a)*: 3.8 scfh emission under intermittently cloudy conditions, with bright sun at the time of recording (64.4 °F, wind speed 2 m/s, 8/22/18 10:54 am).

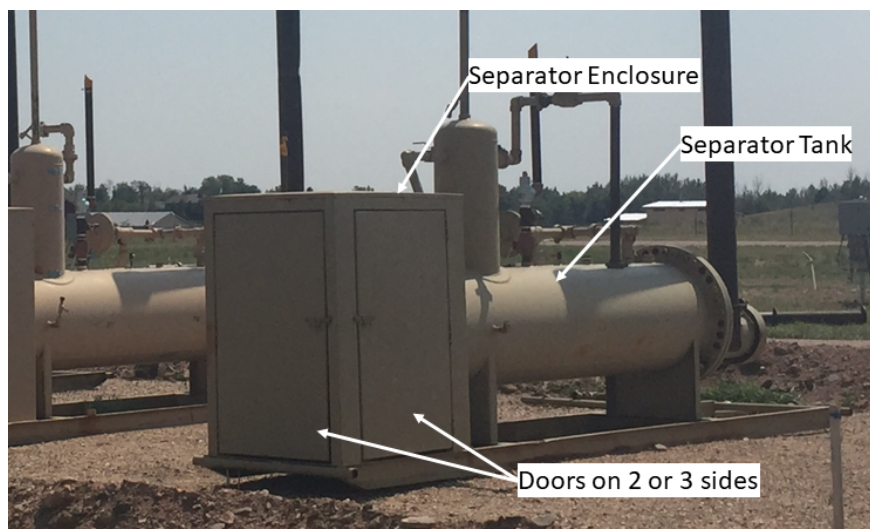


Figure S-23: Photos shows a separator enclosure typical of the surveyor images shown in *SI Video 4*. The enclosure covers the end of the separator and houses pneumatic control components for the separator. The enclosure has two or three doors, depending upon the unit.

- *Description:* Video is a special demonstration video created by the study team (i.e. it was not created by one of the surveyors in the study). The video illustrates method interference in HSM mode potentially caused by direct solar reflection off equipment being observed. Initial frames show emission at close range in auto mode. field of view (FOV) and observation angle is optimized to minimize the specular reflection that later stretches the contrast scale in the view, decreasing detection capability. At about 2 seconds, the camera switches to HSM mode and the surveyor backs away from the emission point, increasing FOV and introducing method interference due to the high contrast from the reflected sunlight. At approximately 17 seconds, surveyor starts moving closer to constrain the FOV, minimizes method interference, and increases detection capability.

S-9 Data Dictionary for Attached Data Files

Affiliation

Detailed organizational affiliation type of the surveyor.

Used in: *Data, SurveyorData*

AffiliationType

Affiliation type - LDAR or Compliance - that was used in analysis.

Used in: *Data, SurveyorData*

AmbientPressure_mbar

Ambient pressure in millibars

Used in: *Data*

AmbientTemperature_C

Ambient temperature in degrees celsius

Used in: *Data*

AproxHeight_m

Approximate height of the emission release point, rounded to even meter values.

Used in: *LeakPointData*

AscendTankCatwalks

Yes' if the surveyor is allowed to ascend catwalks to observe tank vents; 'No' if not.

Used in: *SurveyorData*

ConfigID

Full test identifier, including operator, test ID, pad ID, and day of year. This field can be used to identify all records in the data that correspond to one test configuration surveyed by one operator on a single day.

Used in: *Data*

ConfirmDistance

Distance from the emission point, in feet, when emission was confirmed

Used in: *Data*

ConfirmTimeHigh

Surveyors provided a range of time they used for observing each component when surveying for leaks, in seconds. This field is the high end of the range they provided.

Used in: *SurveyorData*

ConfirmTimeLow

Surveyors provided a range of time they used for observing each component when surveying for leaks, in seconds. This field is the low end of the range they provided.

Used in: *SurveyorData*

Constancy

The time variability of the emission; 'steady' indicates a constant emission rate, 'intermittent' indicates an on/off emission rate, and '-' indicates there was no emission.

Used in: *Data*

Constancy1

Description of the emission point behavior by the surveyor

Used in: *Data*

CriteriaforStoppingSurvey

Surveyor's description of weather conditions under which they would stop a survey. Free form text field.

Used in: *SurveyorData*

DayOfYear

Day of the year; all testing was performed in 2018

Used in: *Data*

Description

Brief description of the component where the emission occurred.

Used in: *Data*

DetectDistance

Distance from the emission point, in feet, when emission was detected.

Used in: *Data*

Detected

Detection code: 'TP' = true positive, 'TN' = true negative, 'FP' = false positive, 'FN' = false negative.

Used in: *Data*

DetectionEndTime

Time at which the detection was confirmed and the surveyor moved on.

Used in: *Data*

DetectionStartTime

For each reported detection, the time when the emission point was first noticed, in fractional hours.

Used in: *Data*

EquipmentCategory

The location where the emission was released or the false positive detected. Valid values include major equipment types – 'Wellhead' (well head casing and associated piping, but not underground leaks nearby), 'Separator' or 'Tank'; 'Ground' for the one leak point located near well heads but underground, 'None' for test configurations with no emission points, and '-' for reported false positives

Used in: *Data*

FormalTrainingType

The study team's interpretation of the certification entity reported by the surveyor in 'TrainingCertification'; Values include 'FLIR' and 'ITC' for those two companies, 'Other' for training programs

from other entities, or no entity listed; 'None' for surveyors who received no formal training, but may have been trained 'on the job' or by organization-internal programs.

Used in: *SurveyorData*

ID

Record identifier. Non-decimal record identifiers indicate a record which was added to the data set during quality assurance checks, and was not reported directly by a surveyor.

Used in: *Data*

InitialScanDistance

Distance from the emission point, in feet, during the initial scan.

Used in: *Data*

InitialSurveyMode

The camera mode the surveyor would normally use during their initial leak survey. Values are: 'High' for high sensitivity mode (HSM); 'Normal' for auto mode; and 'Both' for surveyors who reported using both modes.

Used in: *SurveyorData*

InsideorOutside

Whether the leak was inside or outside of an equipment cabinet

Used in: *Data, LeakPointData*

LocationDescription

Description of the emission location by the surveyor.

Used in: *Data*

METECEmID

METEC emission identifier used to uniquely identify the location where the emission occurred.

Used in: *Data, LeakPointData*

MetConditions

Surveyor's reported meteorological conditions

Used in: *Data*

MethaneDeltaSCFH

Range of the leak rate over the entire test, in scfh methane

Used in: *Data*

MethaneSCFH

Leak rate in scfh methane

Used in: *Data*

MinutesCorrection

If the surveyor completed part of a pad, paused or went to another pad, and then returned to complete the survey, this field provides a correction to the the MinutesOnPad field for time spent away from the pad. Applying this field to the difference between PadStartTime and PadEndTime provides the correct value for MinutesOnPad.

Used in: *Data*

MinutesOnPad

Amount of time the surveyor spent on this pad, during this test configuration.

Used in: *Data*

MinutesPerMajorEquip

MinutesOnPad divided by the count of major equipment - wells, separators and tanks - for that pad

Used in: *Data*

MinutesPerWell

MinutesOnPad divided by the well count for that pad.

Used in: *Data*

NoLeakTest

Whether this report was part of a test configuration that did ('Yes') or did not ('No') have an emisison point on the pad.

Used in: *Data*

Notes

Any notes made by the surveyor

Used in: *Data*

OGISurveysConducted

Surveyor's estimate of the number of surveys conducted prior to the study.

Used in: *SurveyorData*

ObservationHigh

Surveyors provided a range of distances they used for observing equipment for leaks. This field represents the high-end of that range, in ft.

Used in: *SurveyorData*

ObservationLow

Surveyors provided a range of distances they used for observing equipment for leaks. This field represents the low-end of that range, in ft.

Used in: *SurveyorData*

Odor

Indicates of the gas released at the time was odorized.

Used in: *Data*

OpID

Surveyor identifier, which consists of their organization's identification code and a unique number.

Used in: *Data, SurveyorData*

OrgID

Organization identifier, a randomly assigned two-letter code.

Used in: *Data, SurveyorData*

PadEndtime

Time when the survey on the pad ended, in fractional hours.

Used in: *Data*

PadID

Pad identifier – 1 to 3

Used in: *Data*

PadStarttime

Time when the survey on the pad started, in fractional hours.

Used in: *Data*

PrimaryDetectionBackground

Primary detection background for this leak location.

Used in: *Data, LeakPointData*

RainStopCriteria

The study team's interpretation of the rain criteria under which a surveyor would stop a survey. Values are: 'Not Stated' if the survey provided no rain-specific stopping criteria, and 'Yes' if the survey would stop during any appreciable amount of rain.

Used in: *SurveyorData*

RelativeHumidity

Relative humidity

Used in: *Data*

SecondaryDetectionBackground

Secondary detection background for this leak location.

Used in: *Data, LeakPointData*

TestID

Test configuration identifier.

Used in: *Data*

TrainingCertification

Surveyor's certification, as reported by the surveyor. Free form text field.

Used in: *SurveyorData*

TrainingLevel

The study team's interpretation of the certification level reported by the surveyor in 'TrainingCertification'; Levels 1 and 2 correspond to typical training classes for ITC or FLIR thermography training protocols.

Used in: *SurveyorData*

UnobstructedViewingAngle

Unobstructed viewing angle, in degrees from north, for the primary detection direction and primary detection background.

Used in: *Data, LeakPointData*

VideoDistance

Distance from the emission point, in feet, when the accompanying video was captured.

Used in: *Data*

VideoFileID

If available, the video file in the data extended data set.

Used in: *Data*

WholeGasDeltaSCFH

Range of the leak rate over the entire test, in scfh whole gas

Used in: *Data*

WholeGasSCFH

Leak rate in standard cubic feet per hour (scfh), whole gas

Used in: *Data*

WindDirection_deg

Wind direction in degrees from north (north=0)

Used in: *Data*

WindSpeed_ms

Wind speed in m/s

Used in: *Data*

WindStopCriteria_mph

The study team’s interpretation of the criteria under which a surveyor would stop a survey, extracted from ‘CriteriaforStoppingSurvey’ or other information provided by the surveyor to the study team, in miles per hour (MPH); Many surveyors listed the wind speed as ‘high’, and since this could not be assigned to any specific value, it was left as a qualitative ‘high’ term. Some surveyors did not state a specific wind criteria – these are marked as ‘Not Stated’.

Used in: *SurveyorData*

References

- [1] A. P. Ravikumar, J. Wang, M. McGuire, C. S. Bell, D. Zimmerle, and A. R. Brandt, ““Good versus Good Enough?” Empirical Tests of Methane Leak Detection Sensitivity of a Commercial Infrared Camera,” *Environmental Science & Technology*, vol. 52, pp. 2368–2374, Jan. 2018.
- [2] D. T. Allen, V. M. Torres, J. Thomas, D. W. Sullivan, M. Harrison, A. Hendler, S. C. Herndon, C. E. Kolb, M. P. Fraser, A. D. Hill, B. K. Lamb, J. Miskimins, R. F. Sawyer, and J. H. Seinfeld, “Measurements of methane emissions at natural gas production sites in the United States,” *Proceedings of the National Academy of Sciences*, vol. 110, pp. 17768–17773, Oct. 2013.
- [3] C. Bell, T. Vaughn, D. Zimmerle, S. Herndon, T. Yacovitch, G. Heath, G. Pétron, R. Edie, R. Field, S. Murphy, A. Robertson, and J. Soltis, “Comparison of methane emission estimates from multiple measurement techniques at natural gas production pads,” *Elem Sci Anth*, vol. 5, Dec. 2017.